OPEN ACCESS
JOURNAL OF ADVANCED DIELECTRICS
Vol. 12, No. 5 (2022) 2250018 (7 pages)

DOI: 10.1142/S2010135X22500187

Embedding epitaxial VO_2 film with quality metal-insulator transition to SAW devices

M. E. Kutepov[*,§], G. Ya. Karapetyan[*], T. A. Minasyan[*], V. E. Kaydashev[*], I. V. Lisnevskaya[†], K. G. Abdulvakhidov[‡], A. A. Kozmin[*] and E. M. Kaidashev[*]

[*]*Laboratory of Nanomaterials, Southern Federal University, 200/1 Stachki Ave. 344090 Rostov-on-Don, Russia*

[†]*Department of Chemistry, Southern Federal University, 7 Zorge St. 344090 Rostov-on-Don, Russia*

[‡]*Smart Materials Research Institute, Southern Federal University, 178/24 Sladkova St. 344090 Rostov-on-Don, Russia*

[§]kutepov.max@yandex.ru

Received 24 June 2022; Revised 26 August 2022; Accepted 15 September 2022; Published 11 October 2022

Epitaxial VO_2 films grown by pulsed laser deposition (PLD) method with superior phase transition related switching characteristics are successfully embedded to SAW devices using concept of the "impedance loaded SAW sensor". A resistance of VO_2 sensor abruptly drops from 0.7 MΩ to 90 Ω when it is heated above ~65°C and shows a narrow hysteresis loops when switching. Two designs of SAW devices are examined in which RF signal is reflected back from interdigital transducer (IDT) or a surface acoustic waves (SAW) is transferred through a coupler and the RF response is altered 2 and 3 times correspondingly upon the phase transition in VO_2. In the proposed devices with external load, a SAW does not propagate via VO_2 film and therefore is not attenuated which is beneficiary for wireless applications. Additionally, a SAW phase shift as great as 50° is induced to the SAW transferred through the coupler due to the phase transition in VO_2. The proposed approach may boost the development of remotely controlled autonomous sensors, including those based on VO_2 metamaterials and hybrid plasmonic structures for near IR/middle IR and sub-THz/THz applications.

Keywords: Surface acoustic wave; SAW; pulsed laser deposition; PLD; VO_2; epitaxial film.

1. Introduction

Interest to cost-effective surface acoustic waves (SAW)-based wireless autonomous devices has gradually increased recently. Rapid development of information technologies urges design of new types of remotely controlled sensors to monitor various physical quantities including resistance, capacitance, temperature and radiation in all ranges from UV/visible/near IR/middle IR and THz/sub-THz. Moreover, many sensors for gasses, viruses, hazardous bacteria and molecules do also exploit resistance/capacitance alteration. Embedding of all these sensors to SAW devices is highly desired. However, deposition of many functional materials directly on SAW channel faces serious issues. Epitaxial films typically show best characteristics. However, not all high quality epitaxial films may be grown on SAW channel which is normally a special cut of piezoelectric crystal. Also, many sensors with 3D nanostructures such as arrays of nanowires, metal-organic frameworks and others being deposited on acoustic channel often induce dramatic attenuation of acoustic wave which limits or completely damages the device performance.

Instead of depositing a sensing element on acoustic channel, an alternative approach may be exploited, namely, one may load an interdigital transducer (IDT) of a SAW device with sensors impedance. This strategy called "impedance loaded device" allows one to successfully embed many quality functional materials to SAW devices. The efficiency of this approach has already been demonstrated in our patents and recent report on ZnO-based UV SAW photodetector and also was discussed in other studies.[1–6] Briefly, an impedance of a sensor element which is loaded on IDT alters a SAW pulse which is reflected form this IDT. By analyzing the alteration of RF response, one may monitor the target physical quantity which is linked to impedance of a sensor.

VO_2 is well known for its ultra-fast ~26–100 fs switching ability from isolator to metallic state due to its conductivity alteration for more than four orders of magnitude.[7,8] The fast change of the electronic structure and a crystalline phase of VO_2 may be induced by heating above ~68°C, by mechanical stress or by high local electric fields including those due to optical excitation.[7,9–11] A capacitance of VO_2 thin film may be also altered by applying electric bias.[12] Transformed electronic

§Corresponding author.

structure of VO_2 results in its modified UV/visible/near IR and sub-THz/THz photon absorption which makes VO_2 favorable for photodetectors, optically/THz driven switches, switchable SAW splitters, reflectors and photonic devices.[13–15] Besides, more complicated phenomena such as conversion of a near infrared fs-pulse to THz radiation in VO_2 make it prospective for new THz sources.[16] Also, unique properties of VO_2 make it also advantageous for sensing applications.

Thin VO_2 films are fabricated by several methods including DC-magnetron sputtering, sol–gel method, chemical vapor deposition (CVD), molecular beam epitaxy (MBE) and pulsed laser deposition (PLD).[17–26] Discovered PLD regimes allow one to obtain VO_2 film of high crystalline quality which is often favorable for device performance. In particular, a ~10000-fold resistivity alteration was obtained in epitaxial VO_2 films grown on m-Al_2O_3 and on c-Al_2O_3.[25,26] Super abrupt $R(T)$ drop and narrow temperature hysteresis loop in $R(T)$ characteristics with very small ΔT_c of only 1° was also reported for high quality epitaxial films.[26] However, epitaxial VO_2 films are typically grown at elevated temperature of ~630°C and only on a special cut of crystalline substrate, normally sapphire, when materials lattice parameters are best fit. Therefore, a direct growth of quality VO_2 film on a $LiNbO_3$ SAW channel is seriously limited. Thus, embedding of a quality sensor based on epitaxial VO_2 film to SAW device is challenging.

In this paper, we further develop our approach of "impedance loaded" sensor. We show how external sensing element based on high-quality epitaxial VO_2 film preliminarily grown on c-Al_2O_3 substrate may be successfully embedded to SAW-based devices. Two SAW devices where VO_2 sensing element is connected are as follows: (i) Input receiving–transmitting IDT and to (ii) intermediate SAW splitting IDT are examined. The impedance of VO_2 external sensor is gradually altered near isolator-to-metal phase transition which results in significant variation of RF response.

2. Experimental Details

2.1. *Fabrication of VO_2 films*

VO_2 films were prepared on *c*-Al_2O_3 substrates by using PLD method. Radiation of KrF laser (248 nm, 10 Hz) was focused on rotating metallic vanadium target to give fluence of 2.3 J/cm^2. The substrate was positioned at 5 cm from the target and its temperature was stabilized in the range of 600–650°C for different samples. The films were deposited in oxygen ambient at pressure of $3 - 7.5 \cdot 10^{-2}$ mbar for 4000 laser shots. We have experimentally found that films prepared using a protocol with a 5 min pause after the first 500 shots reveal much more abrupt resistance versus temperature characteristics. Therefore, this protocol was applied to all discussed samples. Upon the deposition, the films were kept for 20 min at 650°C and afterwards were cooled down to room temperature in oxygen ambient.

2.2. *Design of SAW devices*

Two types of SAW devices shown in Fig. 1 were fabricated on piezoelectric YX-128° $LiNbO_3$ substrates. Device A is a SAW delay line which consists of receiving–transmitting IDT1 and reflecting IDT2 as shown in Fig. 1(a). Both IDTs contain 17 internal reflectors which are designed to generate SAWs with central frequency of 97.5 MHz. In Device A, resistive sensor based on epitaxial VO_2 film is loaded on the input receiving–transmitting IDT. We showed high effectiveness of monitoring reflection characteristics S_{11} to detect sensors impedance alteration in a similar device in our previous study on impedance loaded ZnO-based UV photodetector.[3] The electric circuit of a sensor was tuned using external inductance coil and capacitor to achieve optimal coupling of sensor with IDT and, thus, obtains best performance.

In Device B, a resistive VO_2 sensor is connected to intermediate SAW splitting IDT, as shown in Fig. 1(b). An acoustic wave incident to this splitting IDT is partially reflected back to input receiving–transmitting IDT and is partially transferred to the second acoustic channel. In such case, the wave is readily transferred from the first to the second acoustic channel only if the resistance of a VO_2 film is compared to 50 Ω. Upon the VO_2 phase transition, the unidirectional IDTs in different delay lines are connected in parallel via small VO_2 resistor. IDTs become well electrically coupled which results in generating a SAW in second acoustic channel. The reflection of incident SAW from coupler becomes minor. When the resistance of VO_2 film is significant, the IDTs are electrically disconnected. Incident SAW is well reflected back to the first channel as it does not transfer to the second channel. In such schematics, the influence of VO_2 resistance

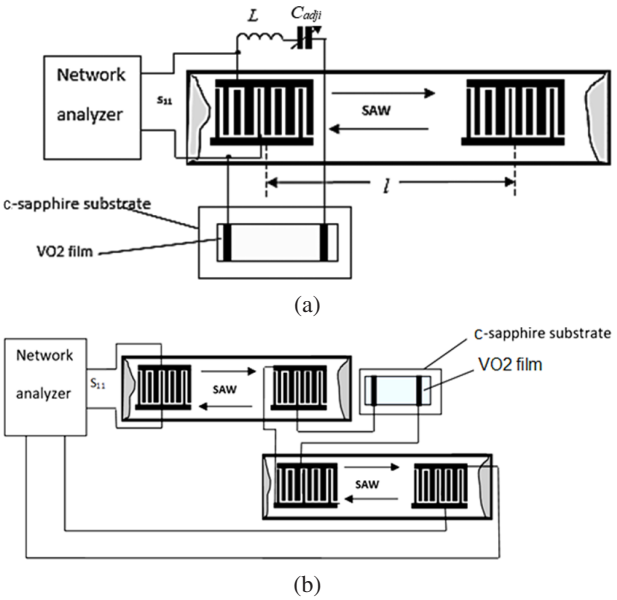

Fig. 1. SAW delay line with impedance of VO_2 film loaded on input receiving–transmitting IDT (a) and on intermediate SAW splitting IDT (b).

on the recorded S_{11} characteristics is greater compared to the device with a single delay line and VO_2 film loaded on reflecting IDT. Indeed, in case of Device B, SAW is shown to have affected in a greater manner by VO_2 films resistance as it passes through the coupler twice when traveling from the input to the receiving–transmitting IDT and back.

S-parameters were recorded by using a network analyzer OBZOR 304/1. The X-ray diffraction (XRD) measurements were carried out using an ARL XTRA diffractometer with CuKα-radiation at 35 kV and 30 mA. The scan step was 0.02°.

3. Results and Discussion

3.1. *Structural properties of VO_2 films*

The XRD pattern of a typical VO_2 film deposited on c-Al_2O_3 substrate shown in Fig. 2 reveals peaks at 39.9° and 86° which correspond to (020) and (040) reflexes of monoclinic VO_2 phase. No other peaks were observed which claims that the films are epitaxial with (010) planes oriented parallel to c-Al_2O_3 substrate. FWHM of (002) and (040) peaks were measured to be as narrow as 0.18° and 0.20°, correspondingly, which claims on a high crystalline quality of prepared films. The unit cell parameter c calculated from the positions of (020) and (040) reflexes is 0.4521 nm which is slightly different from c = 0.4532 nm for monoclinic VO_2 powder sample, exhibiting a minor compressive stress due to film and substrate lattice parameters mismatch.[27]

3.2. *Study of temperature induced resistance alteration in VO_2 films*

The obtained films reveal great switching characteristics with resistance altered for more than three orders of magnitude from 0.7 MΩ to 90 Ω upon the phase transition as shown in Fig. 3(b). The quality of electrical switching properties is well illustrated by the dip in derivative of Log_{10} $R(T)$ value plotted as function of film temperature as shown in Fig. 4. These curves allow one to accurately estimate a number of parameters including phase transition temperature T_{PT}, sharpness ΔT and width ΔH of thermal hysteresis. The parameters of films prepared at optimal deposition conditions are summarized in Table 1.

We have found that the quality of VO_2 film obtained by ablating a metallic vanadium target is heavily dependent on oxygen pressure. To optimize the films characteristics, we first varied oxygen pressure while a temperature of c-Al_2O_3 substrate was chosen to be 600°C. The $R(T)$ characteristics of prepared films are shown in Fig. 3(b). The films deposited at oxygen pressure of 6×10^{-2} mbar reveal greatest 100-fold resistance alteration upon phase transition with typical resistance of ~1 kΩ in high conductivity state. Definitely, the electrical characteristics of best samples obtained at 600°C

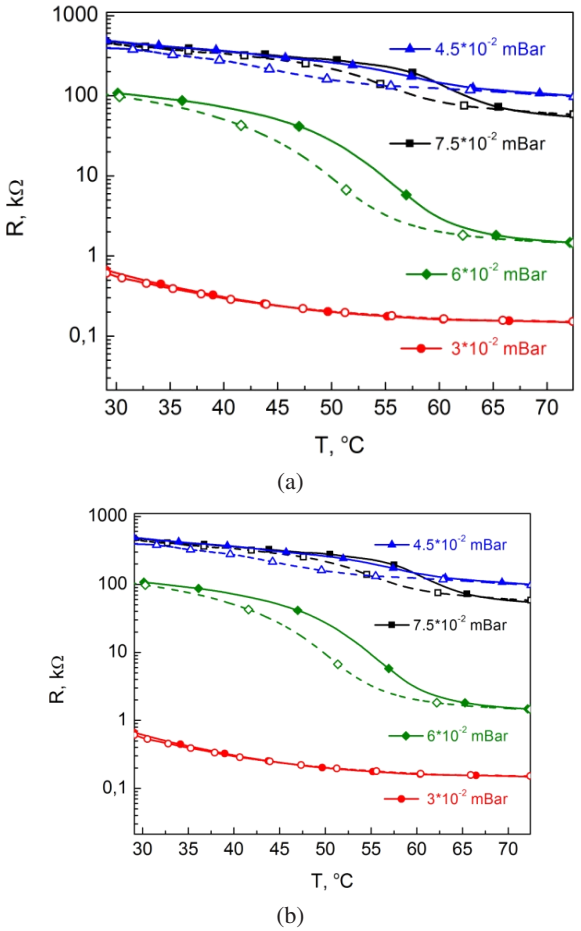

Fig. 3. $R(T)$ curves of VO_2 films grown on c-Al_2O_3 substrates at 600°C and various oxygen pressure; (a) temperature dependent variation of resistance $R(T)$ of VO_2 films deposited on c-Al_2O_3 substrate at 600°C (Sample 1) and 650°C (Sample 2) and at oxygen pressure of 6×10^{-2} mbar (b).

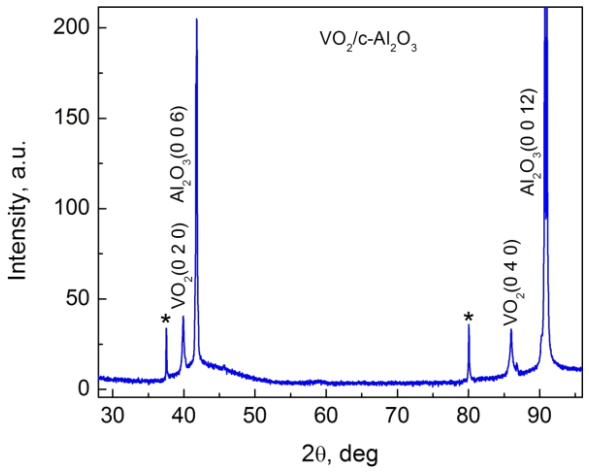

Fig. 2. XRD pattern of VO_2 film on c-Al_2O_3 substrate deposited at 600°C and oxygen pressure of $6\cdot10^{-2}$ mbar; * denotes parasite peaks of a sapphire substrate.

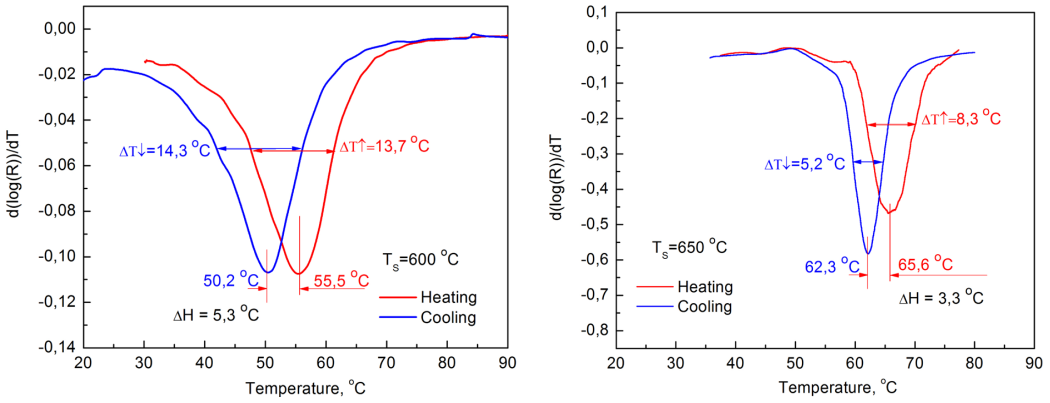

(a) (b)

Fig. 4. Derivatives of $\mathrm{Log}_{10} R(T)$ versus temperature for VO_2 films deposited on c-Al_2O_3 substrate at 600°C (a) and 650°C. (b) and at oxygen pressure of 6×10^{-2} mbar. FWHM of corresponding curves and phase transition points is shown.

Table 1. Synthesis temperature T_s, phase transition temperature T_{PT}, sharpness ΔT, width ΔH of thermal hysteresis, a minimal resistance R_{min} at temperature above phase transition and resistance ratio R_{ratio} of sample in isolator and metal-like states.

Samples	T_s (°C)	T_{PT} (°C)	ΔT (°C)	R_{min} ($k\Omega$)	ΔH (°C)	ΔR_{ratio}
VO_2/c-Al_2O_3 (Sample 1)	600	52.85	14	1.3	5.3	10^2
VO_2/c-Al_2O_3 (Sample 2)	650	63.94	6.7	0.09	3.26	$7.6 \cdot 10^3$

For the transition temperature T_{PT} and sharpness ΔT, the given values are averaged data for heating and cooling curves.

$R(T)$ dependence for Sample 2 deposited at 650°C reveals much higher phase transition temperature and more abrupt resistance drop compared to Sample 1 grown at 600°C as shown in Figs. 3(b) and 4. Resistance of Sample 2 in metallic-like state and a width of heating–cooling hysteresis loop width ΔH are both decreased to be 90 Ω and 3.26°C compared to 1.3 kΩ and 5.3°C for Sample 1. These results are summarized in Table 1.

are not good enough to function as a sensor for a SAW device and further optimization of growth temperature was required. Thus, we fixed the oxygen pressure at 6×10^{-2} mbar and raised temperature to 650°C.

Note that our aim was to find out the deposition protocols to prepare VO_2 films with both abrupt phase transition and narrow temperature hysteresis loop which in addition are optimally embedded to SAW devices A and B. The performance of devices A and B is optimal when the resistance of VO_2 film in conducting state is lower than 100 Ω. Indeed, the reflection of a RF signal from IDT in case of device A or a transfer of a SAW between delay lines in case of device B are both optimal when VO_2 is highly conductive. Sample 2 fits this requirement well.

3.3. *Characterization of SAW devices based on VO_2 film sensor*

An observed significant temperature-dependent alteration of the VO_2 films resistance can be effectively monitored by using SAW devices A and B. In case of Device A equipped with VO_2 film, we tuned the S_{11} characteristics to make it as uniform as possible by adjusting the capacitance of C_{ADJ} in the regime when the film has metallic-like properties (at temperature above phase transition). The optimized shape of the obtained S_{11} characteristics is shown in Fig. 5 in red. In the result of VO_2 films, impedance alteration induced by isolator-to-metal phase transition an amplitude of oscillations in $S_{11}(f)$ characteristics as well as in its Fourier transform $S_{11}(t)$ are more than three times decreased, as shown in Figs. 5(a) and 5(b), correspondingly.

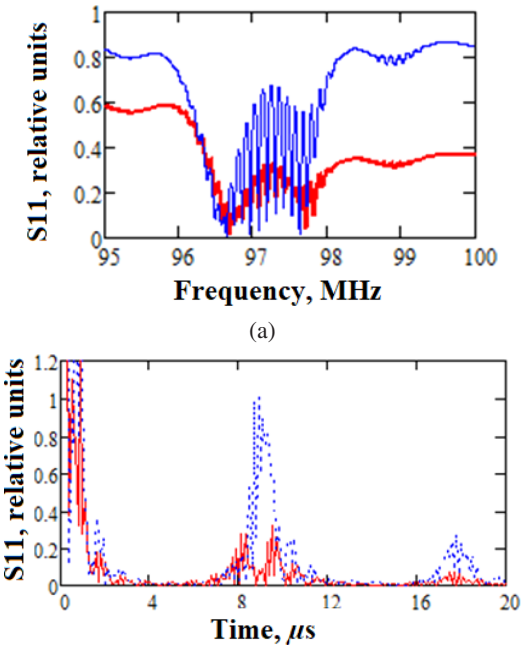

(a)

(b)

Fig. 5. (Color online) S_{11} characteristics of Device A with VO_2 film (Sample 2) loaded on input IDT at VO_2 temperature of 55°C (blue) and at 80°C (red) below and above phase transition, correspondingly (a) and Fourier transforms of S_{11} characteristics (b).

The decreased amplitude of S_{11} characteristics is understood as follows. The impedance of VO_2 film, mainly its conductivity, does influence on the ability of an incident electric signal to generate a SAW in delay line as well as on reflection of incident RF electric signal. Also, the reflection coefficient of SAW incident to IDT1 when it is propagating back from reflecting IDT2 to input IDT1 is also altered, however the input of this effect is minor. More specifically, while a VO_2 film is in isolator-like state a SAW is readily generated in delay line and a SAW reflected from IDT2 is transformed back to electric signal by IDT1. While a VO_2 film is in metallic-like state the RF signal is well reflected from IDT1 back to electric channel and SAW generation is suppressed.

Alternatively, the resistance of obtained VO_2 films was switched due to photothermal effect induced by absorption of near IR light. A continuous laser light at 980 nm was focused on the surface of VO_2 film in Sample 2 to give power density of ~100 mW/cm^2 which is embedded to SAW device A. Sample 1 was additionally heated to 65°C. At this temperature, a VO_2 film is already in the second half of the phase transition and resistance drops to ~200 Ω. However, this resistance is still too high to induce a noticeable alteration of SAW device response. Then, the sample is additionally exposed by IR light the resistance drops to ~90 Ω. The effect of near IR light on S_{11} characteristics of device A is shown in Fig. 6. In contrast to Fig. 5, where an almost complete disappearance of the S_{11} peak was observed, there is no complete attenuation of this S_{11} peak in Fig. 6. Apparently, this is due to the fact that when the film is heated by an IR laser, a temperature of 80°C is not reached.

A Device B with SAW splitting IDT which is coupled/decoupled to acoustic channel shown in Fig. 1(b) also allows one to monitor alteration of VO_2 films resistance. A recorded S_{21} characteristics shown in Figs. 7(a) and 7(b) allows one to monitor an amount of a SAW energy which is transferred from first to second acoustic channel. High conductive state of VO_2 film results in short-cut of two IDTs in SAW channels 1 and 2. Therefore, the amplitude of a SAW transferred from first to second acoustic channels is increased twice. And vice-versa, when a VO_2 film has a large resistance, a coupling of two SAW channels breaks. It is also remarkable that the alteration of VO_2 films results in a phase shift of a SAW in the second acoustic channel as shown in Fig. 7(c). The observed phase shift for ~50° corresponds to SAW velocity altered for 0.016%.

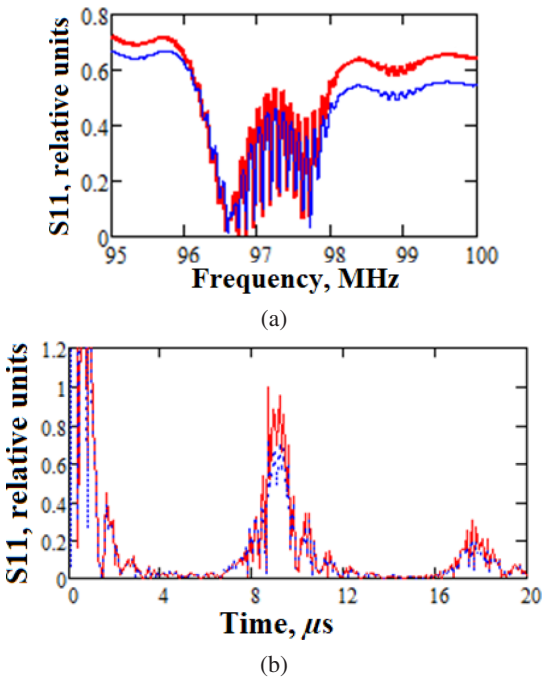

Fig. 6. (Color online) S_{11} characteristics of Device A with VO_2 film (Sample 2) loaded on input IDT at temperature of 65°C in dark (red) and exposed with near IR light (980 nm, ~100 mW/cm^2) (blue) (a) and Fourier transforms of S_{11} characteristics (b).

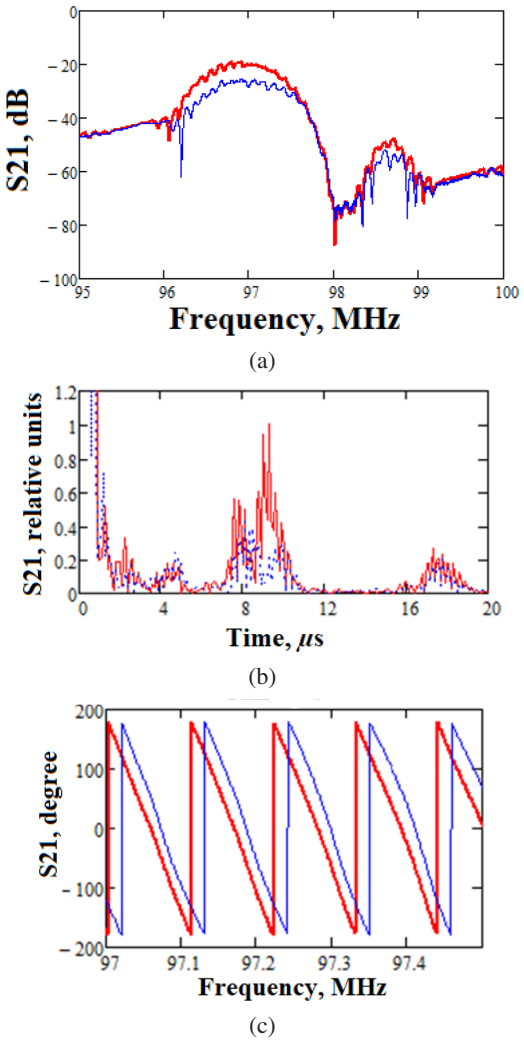

Fig. 7. (Color online) S_{21} characteristics of Device B with impedance of VO_2 film loaded on splitting IDT at VO_2 temperature of 30°C (blue) and at 80°C (red) below and above phase transition, correspondingly (a) and respective Fourier transforms of S_{11} characteristics (b) and phases of S_{21} characteristics (c).

The effect of near IR radiation to Device B is similar to the one discussed above for Device A (not shown here). Therefore, a Device B can also be considered as an efficient splitter of the RF signal controlled by using infrared radiation. Note that an applied approach of external "impedance sensor" is well compatible with higher frequency SAW devices operating at 2.4 GHz. Indeed, a SAW is not propagating inside a sensing element and, thus, is not attenuated, allowing precise monitoring of sensors impedance.

4. Conclusions

We have implemented a concept of the "impedance loaded SAW sensor" to embed a high quality epitaxial VO_2 film to SAW devices. The VO_2 sensor being the external load outside the acoustic channel does influence on the RF signal reflection from IDT or SAW transfer to another channel however not attenuating a SAW which is beneficiary for wireless applications. Electrical characteristics alteration induced by phase transition in VO_2 film were optimized by varying oxygen ambient pressure and growth temperature to meet requirements for embedding of a sensor to SAW device. Best epitaxial VO_2 films grown by our PLD protocol show great switching characteristics with resistance altered from ~0.7 MΩ to ~90 Ω and narrow $R(T)$ hysteresis loop. We have characterized two SAW devices in which VO_2 sensing element is connected to input receiving–transmitting IDT or to intermediate SAW splitting IDT in which the response is altered more than three times or more than twice correspondingly upon phase transition in VO_2. Also, a 50° SAW phase shift is observed for SAW transmitted through the coupler. Additionally, the proposed devices were shown to operate as near IR photodetectors/optically controlled RF splitters which are prospective building blocks for smart wireless applications. We believe that the proposed approach will boost the development of remotely controlled autonomous sensors, including those based on VO_2 metamaterials and hybrid plasmonic structures for near IR/middle IR and sub-THz/THz applications including 6G communication technology.

Acknowledgments

This study is supported by Southern Federal University research project No.07/2020-06-MM and 10th Anniversary International Conference on "Physics and Mechanics of New Materials and Their Applications" (PHENMA 2021–2022).

References

[1]A. S. Bagdasarian, S. A. Bagdasarian, U. V. Gulyaev and G. Ya. Karapetyan, Sensor for remotely controlling physical value on surface acoustic wave, February 03 2004. Patent RF 2296950.

[2]A. S. Bagdasarian, S. A. Bagdasarian, G. Ya. Karapetyan and V. G. Dneprovskii, Sensor of Physical Value on Surface Acoustic Waves, 04 2010. Patent RF 2387051.

[3]G. Y. Karapetyan, V. E. Kaydashev, D. A. Zhilin, M. E. Kutepov, T. A. Minasyan and E. M. Kaidashev, A surface acoustic wave impedance-loaded high sensitivity sensor with wide dynamic range for ultraviolet light detection, *Sens. Actuat. A Phys.* **296**, 70 (2019).

[4]Q. Fu, H. Stab and W. J. Fischer, Wireless passive SAW sensors using single-electrode-type IDT structures as programmable reflectors, *Sens. Actuat. A Phys.* **122**, 203 (2005).

[5]L. Reindl, Theory and application of passive saw radio transponders as sensors, *IEEE Trans. Ultrason. Ferroelectr. Frequency Control* **45**, 1281 (1998).

[6]W. Luo, Q. Fu, J. Wang, Y. Wang and D. Zhou, Theoretical Analysis of Wireless Passive Impedance-Loaded SAW Sensors, *IEEE Sensors Journal*, **9**, 1778 (2009).

[7]A. Cavalleri, Th. Dekorsy, H. H. W. Chong, J. C. Kieffer and R. W. Schoenlein, *Phys. Rev. B* **70**, 161102(R) (2004).

[8]M. Borek, F. Qian, V. Nagabushnam and R. K. Singh, Pulsed laser deposition of oriented VO_2 thin films on R-cut sapphire substrates, *Appl. Phys. Lett.* **63**, 3288 (1993)

[9]D. Y. Lei, K. Appavoo, F. Ligmajer, Y. Sonnefraud, R. F. Haglund and S. A. Maier, Optically-triggered nanoscale memory effect in a hybrid plasmonic-phase changing nanostructure, *ACS Photon*. **2**, 1306 (2015).

[10]J. Wei, Z. Wang, W. Chen and D. H. Cobden, New aspects of the metal-insulator transition in single-domain vanadium dioxide nanobeams, *Nat. Nanotechnol*. **4**, 420 (2009).

[11]M. M. Qazilbash, Z. Q. Li, V. Podzorov, M. Brehm, F. Keilmann, B. G. Chae, H. T. Kim and D. N. Basov, Electrostatic modification of infrared response in gated structures based on VO_2, *Appl. Phys. Lett.* **92**, 241906 (2008).

[12]V. S. Aliev, S. G. Bortnikov and I. A. Badmaeva, Anomalous large electrical capacitance of planar microstructures with vanadium dioxide films near the insulator-metal phase transition, *Appl. Phys. Lett.* **104**, 132906 (2014).

[13]J. M. Wu and W. E. Chang, Ultrahigh responsivity and external quantum efficiency of an ultraviolet-light photodetector based on a single VO_2 microwire, *ACS Appl. Mater. Interfaces* **6**, 14286 (2014).

[14]Q. He, Sh. Sun and L. Zhou, Tunable/reconfigurable metasurfaces: Physics and applications, *AAAS Res*. **2019**, 1849272 (2019).

[15]Z. Song, A. Chen and J. Zhang, Terahertz switching between broadband absorption and narrowband absorption, *Opt. Exp.* **28**, 2037 (2020).

[16]N. A. Charipar, H. Kim, S. A. Mathews and A. Piqué, Broadband terahertz generation using the semiconductor-metal transition in VO_2, *AIP Adv*. **6**, 015113 (2016).

[17]A. Lafort, H. Kebaili, S. Goumri-Said, O. Deparis, R. Cloots, J. De Coninck, M. Voué, F. Mirabella, F. Maseri and S. Lucas, Optical properties of thermochromic VO_2 thin films on stainless steel: Experimental and theoretical studies, *Thin Solid Films* **519**, 3283 (2011).

[18]J. B. K. Kana, J. M. Ndjaka, P. O. Ateba, B. D. Ngom, N. Manyala, O. Nemraoui, A. C. Beye and M. Maaza, Thermochromic VO_2 thin films synthesized by rf-inverted cylindrical magnetron sputtering, *Appl. Surf. Sci*. **254**, 3959 (2008).

[19]T. Driscoll, H.T. Kim, B. G. Chae, M. Di Ventra and D. N. Basov, Phase-transition driven memristive system, *Appl. Phys. Lett.* **95**, 043503 (2009).

[20]S. Mathur, T. Ruegamer and I. Grobelsek, Phase-selective CVD of vanadium oxide nanostructures, *Chem. Vap. Depos*. **13**, 42 (2007).

[21]M. B. Sahana, M. S. Dharmaprakash and S. A. Shivashankar, Microstructure and properties of VO_2 thin films deposited by MOCVD from vanadyl acetylacetonate, *J. Mater. Chem.* **12**, 333 (2002).

[22]L. Dillemans, R. R. Lieten, M. Menghini, T. Smets, J. W. Seo and J. P. Locquet, Correlation between strain and the metal-insulator transition in epitaxial V_2O_3 thin films grown by molecular beam epitaxy, *Thin Solid Films* **520**, 4730 (2012).

[23]A. D. Rata, A. R. Chezan, M. W. Haverkort, H. H. Hsieh, H. J. Lin, C. T. Chen, L. H. Tjeng and T. Hibma, Growth and properties of strained VO_x thin films with controlled stoichiometry, *Phys. Rev. B. Condens. Matter Mater. Phys*. **69**, 075404 (2004).

[24]S. Fan, L. Fan, Q. Li, J. Liu and B. Ye, The identification of defect structures for oxygen pressure dependent VO_2 crystal films, *Appl. Surf. Sci*. **321**, 464 (2014).

[25]B. J. Kim, Y. W. Lee, S. Choi, B. G. Chae and H. T. Kim, Analysis of the surface morphology and the resistance of VO_2 thin films on M-plane Al_2O_3, *J. Korean Phys. Soc*. **50**, 653 (2007).

[26]D. H. Kim and H. S. Kwok, Pulsed laser deposition of VO_2 thin films, *Appl. Phys. Lett*. **65**, 3188 (1994).

[27]J. Galy and G. Miehe, Ab initio structures of (M2) and (M3) VO_2 high pressure phases, *Solid State Sci*. **1**, 433 (1999).